MAPPING HYDROTHERMAL ALTERATION ZONES IN THE DIDINGA HILLS, SOUTH SUDAN.

Cosmas Kujjo[1], Liang Liang[2], Dhananjay Ravat[1].
1 Earth and Environmental Sciences, University of Kentucky, 101 Slone Building, Lexington, KY 40506, USA
2 Department of Geography, University of Kentucky, 801 Patterson Office Tower, Lexington, KY 40506, USA

Abstract

South Sudan, a new country, is planning to develop its mineral sector by allocating exploration licenses to investors, a decision that requires preliminary knowledge of the geology and mineral occurrences, both of which are un available as the country has been engaged in a civil war for over 50 years. In concert with this need, the objective of this study is to apply remote sensing techniques for mapping hydrothermal alteration zones of the Didinga Hills region in South Sudan, an area that is not easily accessible due to rugged terrain, poor roads, and wars; hence the mapped alteration zones would be utilize as potential areas to facilitate allocation of mineral titles through the South Sudan Mining Cadastre System. Despite that, there are artisanal gold mining sites being excavated by the natives in the area for decades. Those sites have been utilized as ground truth in verifying the results of this study. Digital processing of the multispectral images (Landsat 8) for the study area has been performed to extract information related to lithology, hydrothermal alteration, and geological structures using optimal band combination, band ratioing, and principal component analysis techniques. The results proved the efficiency of remote sensing data and techniques in providing the required geological information for the new country to sustainably develop its crucial mineral resources, which will contribute effectively to socioeconomic planning, development, and prosperity of the nation.

3.1 Introduction

Geologic mapping through in situ field survey is tedious, time consuming, expensive, and sometimes impractical, especially in remote and rugged terrain areas and war-affected regions. Such limitations could be mitigated by utilizing satellite remote sensing, which is not restricted by the natural and social barriers on the ground.

Geologic mapping is widely used in planning exploration strategies, such as the selection of regions to explore and extract certain types of ore deposits [1]. Mapping of hydrothermal alteration zones, ore minerals, igneous rocks hosting ores, and oxidized and leached rocks that commonly occur at the surface above sulfide-bearing ores can be used in conjunction with geophysical and geochemical data to produce zonation patterns to define prospective corridors of exotic mineralization [1]. Likewise, regional mapping of major faults or contacts bounding shear zones that coincide with a map-scale transition from green schist to amphibolite facies regional metamorphism are spatially associated with major gold deposits in Archean greenstone belts; hence are considered to indicate areas of enhanced exploration potential [2] [1].

South Sudan, a new country separated from Sudan in 2011, is planning to allocate exploration licenses to investors, a decision that requires preliminary knowledge of locations of mineral resources. Similarly, construction of its major infrastructure, e.g. capital city, dams, roads, and bridges, requires geological information about sites, hazards, and building materials. In concert with this need, the objective of this study is to apply remote sensing techniques for mapping hydrothermal alteration zones of the Didinga Hills region in South Sudan; hence utilize the mapped alteration zones as potential areas to facilitate allocation of mineral titles through the South Sudan Mining Cadastre System.

The Didinga Hills are located in the southeastern part of the country and borders Uganda, Kenya, and Ethiopia (Fig. 1), an area that is not easily accessible due to rugged terrain, poor roads, and wars (e.g., due to unexploded land mines). We selected Didinga Hills as the study area for testing remote sensing techniques because of the region's diverse geology, aridity and bedrock surface exposure relative to other parts of the country that are occupied by rain forest. The region is also ideal for this project because it is known for exploration of alluvial gold. Although the bedrock source to the alluvial gold has not been established, but there is clear field association between the presence of the alluvial gold workings in the study area and the background geology of metasediments, schists, marble, and younger post-tectonic granitic intrusions known to cause contact metamorphism and alteration, as well "unpublished" [3].

Remote sensing offers a synoptic view on a regional scale, hence providing a complementary perspective to ground observations. In 2002, Ariki et al., carried out a reconnaissance fieldwork project (funded by the United States Agency for International Development, USAID) in the area during which **mapping** of only 60 sq. km was accomplished in several months. Consequently, this study aims at utilizing remote sensing for mapping hydrothermal alteration zones of

the Didinga Hills region to obtain better coverage and accuracy with significantly reduced time and cost.

Figure 1. Location map of the study area (Modified from www.nationsonline.org)

Hydrothermally altered rocks are characterized by unusually colorful appearances. The various colorful rocks are the host rocks of those mineral deposits with the colors representing the results of chemical interaction with the surrounding hydrothermal fluids [4]. The hydrothermal fluid processes altering the mineralogy and chemistry of the host rocks can produce distinctive mineral assemblages which vary per the location, degree, and duration of those alteration processes. When these alteration products are exposed at the surface, they can be mapped as a zonal pattern, theoretically concentric around a core of highest grade alteration and greatest economic interest [5].

Although gold cannot be detected directly by any remote sensing method, the presence of minerals such as iron oxides and clay minerals, whose diagnostic spectral signatures, (in the visible/shortwave infrared portion of the electromagnetic spectrum) could be used as indicators for identification of hydrothermal alteration zones, which are associated with gold occurrences "unpublished" [6] [7]. Hence, knowledge of these mineral occurrences facilitates the licensing process which is of prime importance in the exploitation of the country's mineral resources.

3.2 Regional geological setting

The area is part of the Precambrian East African Orogeny comprising the Arabian-Nubian Shield (ANS) in the north and the Mozambique belt in the south [8] and is dominated by volcano-sedimentary rocks, dismembered ophiolites, and syn- and post-tectonic granitoids. There are occurrences of many rejuvenated older crustal terranes and accumulations of sediments and/or volcanic rocks in aulacogens or basins, which subsequently were metamorphosed and deformed. The final accretion of different island arcs resulted in strong tectonic deformation during the Pan-African orogeny in the Neoproterozoic.

In the study area, there are Archean cratonic rocks of high-grade metamorphism (granulites), (e.g., the Imatong Mountains) the Proterozoic granitoids, meta- sedimentary, and meta-volcanic rocks (Fig. 2). The metamorphic basement is poorly surveyed and so is shown as undifferentiated (i.e., not separately identified or distinguished) basement on existing maps. Likewise, there are insufficiently structural studies or modern age determinations on the basement rocks to allow a viable subdivision into major tectonic units or terranes [9].

Overlying the basement rocks are effusive volcanic rocks (mainly basalts) that occupy the eastern border areas with Kenya and Ethiopia. These volcanic rocks are related to the East African Rift System (EARS). These in turn are overlain by the Tertiary to Quaternary unconsolidated sediments (Umm Ruwaba Formation) which are mainly sands, gravels, clay sands, and clay "unpublished" [3] [10]. The altitude varies between 440 m and 3100 m. Hence, many seasonal streams flow down the hills, causing remarkable erosion that leads to widespread deposition of placer gold, along with eluvial and alluvial stream sediments.

There are widespread artisanal gold mining sites being excavated by the natives in the area for decades (Fig. 3).

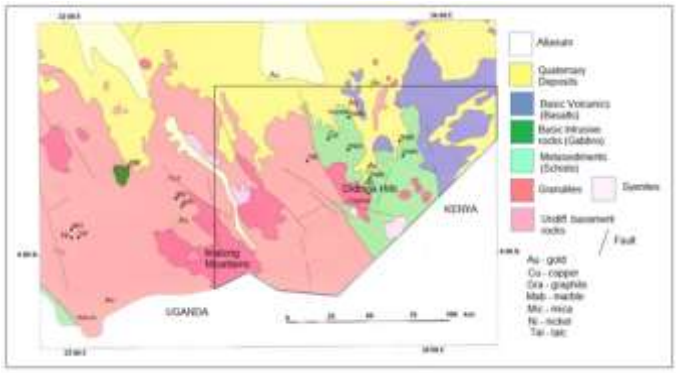

Figure 2. Geological Map of the Kapoeta mineral district with study area demarcated
(Modified from BGS International, UK).

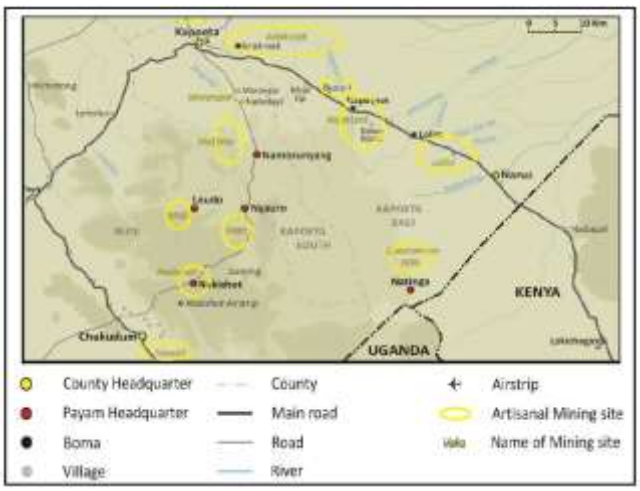

Figure 3. Artisanal gold mining sites in the study area.

3.3 Methodology

The multispectral imagery for the target area is comprise of one frame of Landsat 8 data (P171/R057), collected on January 10th, 2015. The visible (VIS) and shortwave infrared (SWIR) Bands 1 to 7 and 9, in addition to the thermal infrared (TIR) bands 10 and 11 of Landsat 8 were stacked and used in this study. The TIR were resampled to 30m spatial resolution. The SWIR bands are useful in rock and mineral discrimination, whereas TIR are useful in recognizing silicate minerals. Table 1 below shows a list of both Landsat 7 and Landsat 8 bands with their wavelength coverage and pixel size, as well.

Table 1. list of both Landsat 7 and Landsat 8 bands
Landsat-7 ETM+ Bands (µm)Landsat-8 OLI and TIRS Bands (µm)

Landsat-7 ETM+ Bands (µm)		Landsat-8 OLI and TIRS Bands (µm)	
		30 m Coastal/Aerosol 0.435 - 0.451	Band 1
Band 1	30 m Blue 0.441 - 0.514	30 m Blue 0.452 - 0.512	Band 2
Band 2	30 m Green 0.519 - 0.601	30 m Green 0.533 - 0.590	Band 3
Band 3	30 m Red 0.631 - 0.692	30 m Red 0.636 - 0.673	Band 4
Band 4	30 m NIR 0.772 - 0.898	30 m NIR 0.851 - 0.879	Band 5
Band 5	30 m SWIR-1 1.547 - 1.749	30 m SWIR-1 1.566 - 1.651	Band 6
Band 6	60 m TIR 10.31 - 12.36	100 m TIR-1 10.60 - 11.19	Band 10
		100 m TIR-2 11.50 - 12.51	Band 11
Band 7	30 m SWIR-2 2.064 - 2.345	30 m SWIR-2 2.107 - 2.294	Band 7
Band 8	15 m Pan 0.515 - 0.896	15 m Pan 0.503 - 0.676	Band 8
		30 m Cirrus 1.363 - 1.384	Band 9

The geological map of the region (Fig. 2) shows all lithologic units for utilization as ground reference to aid interpretation of the processed satellite imagery of the study area. Likewise, known artisanal gold mining sites (Fig. 3) can be matched with the hydrothermal alteration sites identified by the analysis of the multispectral images. Digital processing of the multispectral images for the study area was performed using ERDAS Imagine and ER Mapper software (Hexagon AB).

Over the past two decades, the development of spectral remote sensing technologies has significantly advanced capabilities for mapping mineral system-related alteration, particularly with the applications of hyperspectral remote sensing data [11]. However, a long-standing problem in remote sensing has been the trade-off between the ability to map complex scenes and the expense of developing sensors with high Signal-to-Noise Ratio (SNR) and spatial/spectral resolution [12]. Currently, the operational hyperspectral remote sensing data (e.g. AVIRIS, HyMap, Hyperion) are difficult to apply to a wide area because of the relatively narrow swath compared to Landsat ETM [13].

Hydrothermal alteration minerals with diagnostic spectral absorption properties in the visible and near-infrared (VNIR) through the shortwave infrared (SWIR) wave length regions can be identified by multispectral and hyperspectral remote sensing data [14].

One of the key idea of remote sensing techniques in exploration geology is that it is applied to rocks, minerals, and structures associated with a particular ore, and not the ore itself. There are very logical reasons for this procedure. The ore is not always exposed at the surface, and it is often not as spectrally unique or as widely disseminated as the minerals and rocks that are associated with the ore body [7].
The multispectral image processing techniques selected and applied in this research included:
1) Optimal color composite with the selection of the optimal band combinations based on the Optimum Index Factor (OIF) developed by Chavez et al. [15]; 2) Spectral ratio techniques [7]; and 3) Principal Component Analysis (PCA) described by Crosta and Moore [16]. These techniques are further discussed below.

3.1 Optimal color composite images

Generation of a composite image has been done by blending information from three selected bands based on their relation to known spectral properties of rocks and alteration minerals [7] [17]. For instance, in Landsat 7, the SWIR band 7 is useful in rock and mineral discrimination [7] [18] [17].

Spectral analysis of remote sensing imagery exploits variation in color intensity values within color composite images to interpret them in terms of lithological variations and/or rock alterations; thus, the choice of bands to generate a composite image is site dependent. The best combinations of spectral bands for lithologic discrimination were determined using the Optimum Index Factor (OIF) [15].

$$OIF = \sum_{i=1}^{3} S_i \Big/ \sum_{i \neq j;\, j=1}^{3} |R_{ij}| \quad (1)$$

where Si is the standard deviation for band i, Rij is the correlation coefficient between bands i and j of the three bands being evaluated.
Finally, the OIF values are ranked in a table in a descending order.

The relative order of the three bands into three colors of Red, Green, and Blue (RGB) has no effect on the value of OIF [15]. The OIF computation simplifies the complex and tedious process of selecting three appropriate bands to combine in colors for optimum interpretation. However, the technique is scene dependent and suffers from non-uniformity of images due to assignment of colors based on the determination of the analyst [19].

3.2 Band ratioing

Band ratioing is a technique used for the effective display of spectral variations [20] [21] and hence enhances compositional information while suppressing other types of information about the earth's surface, e.g., terrain slope and grain size differences [7]. Band ratioing means dividing the pixel values in one spectral band by the corresponding pixel values in a second band. The reason for this is twofold. First, the differences between the spectral reflectance of certain surface types can be highlighted or emphasized. The second reason is to remove the variation caused by differences in illumination, and consequently radiance which may affect interpretation; Consequently, the ratio between differentially illuminated area of the same surface type will be homogenized [7] [17]. Overall, this process enhances the contrast between materials by dividing the brightness values (digital numbers, DN) of two selected bands [22] [7], because shadows are regions of greatly reduced radiance in all spectral bands.

Choice of band ratios depends on the purpose of the application, spectral reflectance, and positions of the absorption bands of the mineral being mapped. For discrimination of alteration of clay minerals (e.g. AlOH), Landsat 8 ratio B6/B7 is generally preferred, whereas for iron oxide minerals (e.g. gossans, limonite, and hematite) the ratio B4/B2 which characteristically displays bright signatures for iron oxides. The ratio B5/B6 emphasizes ferrous minerals [23].

Different alteration assemblages create outcrops of different morphology. For instance, silica-pyrite alteration produces resistant cliff outcrops, whereas clay-rich alteration assemblages result in extensive colluvium [24]. The band ratio technique addresses well the influence of topography on spectral response, which qualifies it as one of the effective methods for mapping hydrothermally altered rocks.

3.3 Principal Component Analysis (PCA) Transformation

Image transformation based on PCA is an image enhancement technique for displaying the maximum contrast from multiple spectral bands with just three primary composite bands [7]. PCA is a multivariate statistical technique used to reduce data redundancy by transforming the original data into new orthogonal principal component axes producing uncorrelated images. Such an image set has much higher contrast than the original bands.

The number of output principal component (PC) bands are equal to the input spectral bands, with the first principal component, PC1, containing most of the data variability [25]. Each subsequent PC contains the next highest amount of variance, which becomes smaller as the order of the PC increases [7]. The last PC bands contain least variance and represent the most unusual, most distinctive pixels in the scene. Some of those distinctive pixels are noise, which often can be recognized as such by noticing their distinctive spatial patterns. The remaining distinctive pixels are the rarest minerals in the frame or scene, though we cannot identify the mineral composition by PC images alone.

The PCA technique applied for the data in this paper was introduced by Crosta and Moore (1989) essentially based on the examination of PCA eigenvectors to determine which PC images concentrate information directly related to the theoretical spectral signatures of specific targets. The relevant PC images could then show targeted surface types (rock, soil, and vegetation) by highlighting them as bright or dark pixels, depending on their respective eigenvector magnitudes and signs (positive/negative). The Crosta and Moore technique can be implemented to delineate hydrothermal alteration zones [26].

In the current study, a variation method based on the PCA, called Feature-oriented Principal Component Selection (FPCS), was applied in processing of Landsat 8 imagery to extract hydrothermal alteration zones. The technique uses the generalized reflectance curve of the feature of interest, such as hydrothermal alteration in which band ratios are considered in the choice of the best Principal Component, based on the ratio of their respective eigenvector values "unpublished" [6].

The FPCS technique is performed by using four selected Operational Land Imager (OLI) bands to highlight the spectral response of iron-oxide minerals (absorption in VIS bands 2 and higher reflection in the VIS Band 4 (in case of Landsat 8) and hydroxyl-bearing (clay) minerals (absorption in SWIR band 7, higher reflectance in SWIR band 6). For instance, to determine which PC best represents iron-bearing minerals depends on the eigenvector values of bands 4 and 2 in a Landsat 8 dataset. Likewise, the representation of clay minerals is controlled by the eigenvectors of bands 6 and 7 referenced to their generalized reflectance spectra curve of the USGS Library of minerals [26].

The signs (+/-) of the eigenvector values was considered in the ratioing process because they determine which feature of interest (Fe oxide or clay) would be represented as bright or dark pixels in the image. In selecting the optimum principal component, the two eigenvector values should always be different in signs. Consequently, the numerator being positive implies bright pixels, whereas when it is negative im-

plies dark pixels representing the feature of interest [26] [27] [28].

4. Results and Interpretations

Band combination using the OIF in selecting the best spectral bands based on their contrast was effective. The true color image with the combination of bands 4, 3, 2 in RGB (Fig. 4) is among the least contrast images, whereas the false color combination of bands 4, 7, 5 in RGB (Fig. 5) exhibit greater contrast and hence more variety of lithologies are displayed in accordance with the respective OIF.

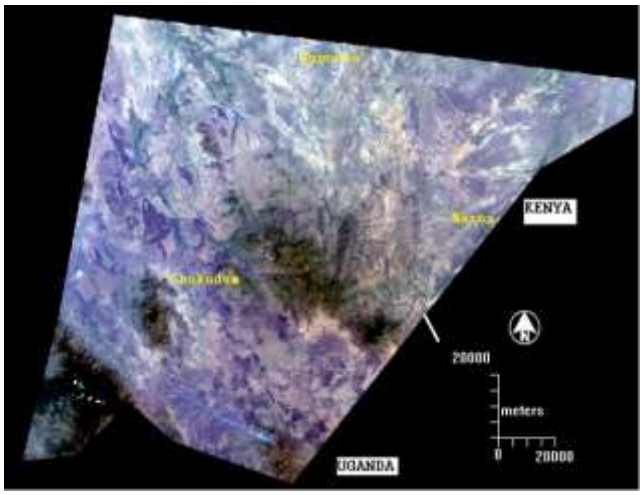

Figure 4. Simulated true color image of the Didinga Hills formed with the combination of bands 4, 3, and 2 assigned to the red, green, and blue colors (RGB), respectively.

This band combination (FCC 432 RGB) is as close to "true color" as one can get with a Landsat OLI image. One unfortunate drawback with this band combination is that these bands tend to be susceptible to atmospheric interference, so they sometimes appear hazy, such as the smoke trending NW in the lowest corner of Figure 4 above.

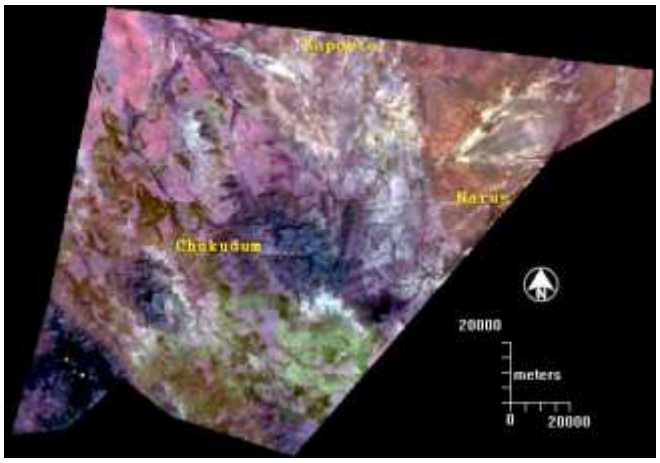

Figure 5. FCC Image 475 RGB of the Didinga Hills for better lithological identification.

Band ratio image OLI B4/B2 highlights rocks that have been subjected to oxidation of iron-bearing sulfides (e.g. pyrite and chalcopyrite). This is because altered rocks are more reflective in Band 4 and less reflective in Band 2 – the latter because of iron absorption [23] [7] [29] [17]. Likewise, the ratio for the clay alteration B6/B7 revealed brighter pixels over rock exposures mostly of the undifferentiated Precambrian basement. The intensity of alteration gradually changes for the gray images from darker (fewer) to brighter (more) tones.

In color composite images, the variation depends on the color assignment. On the other hand, in the ratio image (Fig. 6), the red color has been assigned to the ratio B4/B2, the green to B6/B5, and the blue to B6/B7, respectively. The result is that the areas of hydrothermal alteration appear as bright yellow.

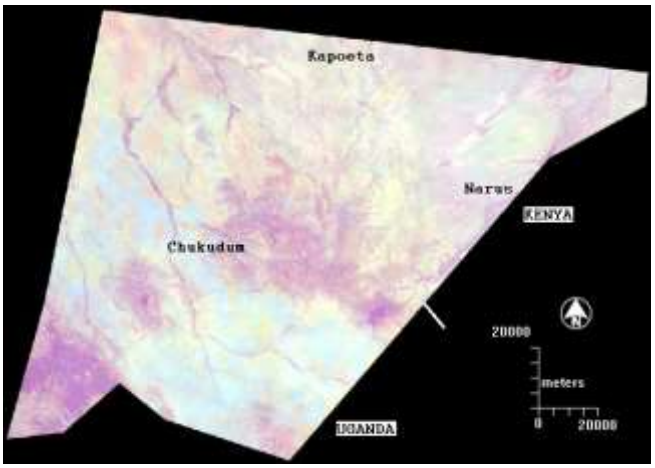

Figure 6. Color combination of the band ratio images B4/B2, B6/B5 and B6/B7 assigned to red, green and blue colors, respectively. Hydrothermal alteration zones appear as bright yellow (almost equal amounts of displayed colors of red and green).

For Feature-oriented Principal Component Selection (FPCS), statistical calculations of Landsat 8 image for the Didinga Hills region have produced the required parameters for data input, which are then used to determine the targeted alteration type and the relative PC number, and whether it would be represented as a bright or dark pixel in the resulting image.

The selected bands are shown in Tables 2 and 3 below.

Table 2. Feature oriented Principal Component Selection (FPCS) data (Bands 2, 4, 5, and 6) for Iron oxide minerals.

Eigenvector	Band 2	Band 4	Band 5	Band 6
PC 1	0.500	0.502	0.497	-0.501
PC2	-0.457	-0.415	0.780	0.098
PC 3	-0.521	0.097	-0.351	0.772
PC 4	-0.518	0.753	0.144	-0.380

Table 3. Feature oriented Principal Component Selection (FPCS) data (Bands 2, 5, 6, and 7) for clay minerals.

Eigenvector	Band 2	Band 5	Band 6	Band 7
PC 1	0.500	0.500	0.500	0.500
PC2	-0.598	-0.388	0.540	0.447
PC 3	0.626	-0.770	0.124	0.019
PC 4	0.007	-0.083	-0.666	0.742

The highlighted values in Tables 2 and 3 shows that iron alterations appear as bright tones pixels in PC4 (Fig. 7) because eigenvector values are positive for band 4 and negative for band 2. Thus, the iron alteration ratio B4/B2 will appear as bright. Contrarily, the eigenvector values are negative for band 6 and positive for band 7, which implies that the clay alteration ratio B6/B7 will be represented in PC4 by dark pixels (Fig. 8).

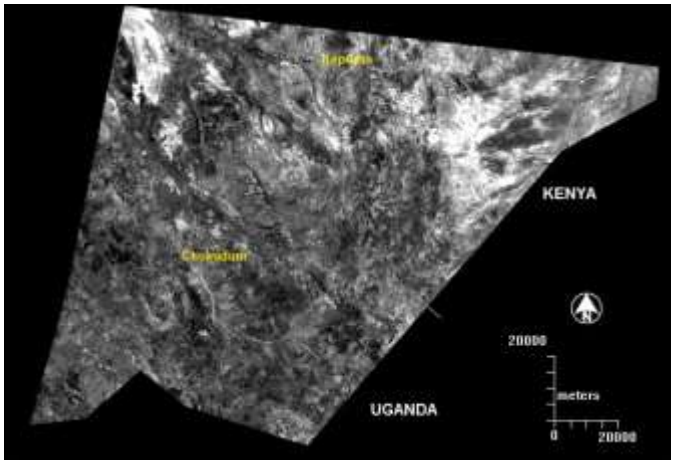

Figure 7. PC 4 (Bands 2,4,5,6) showing iron oxide alterations as pixels of bright tones.

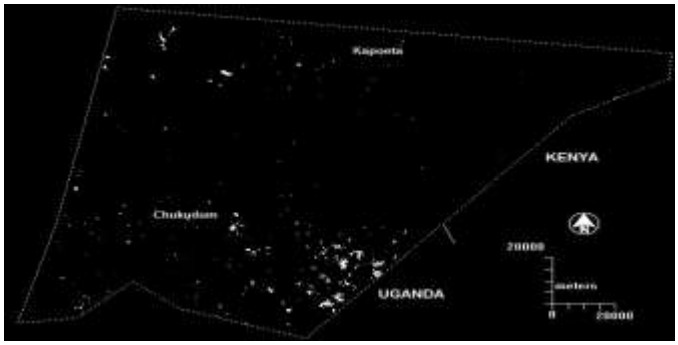

Figure 8. PC 4 (Bands 2,5,6,7) showing clay alteration minerals as dark pixels because eigenvector values of the numerator (band 6) is negative. See the principal component analysis methods section. Gradation within the dark pixels is difficult to observe and therefore it's coloring pattern is reversed in Figure 9.

The enhancement to the clay (hydroxyl-bearing) alteration minerals were obtained after their respective PC4 was made positive (DN multiplied by -1), such that these alteration minerals would be mapped in brighter and distinguishable tones (Fig.9). The clay minerals cover a wide area, especially on low-lying plains in the southern part of the study area.

Those areas are not necessarily representing potential mineral prospect locations, but instead are only the accumulation of muds deposited by flash floods.

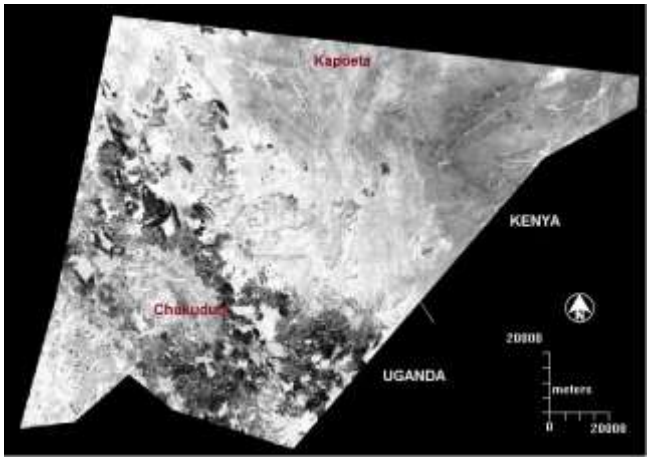

Figure 9. Clay minerals alteration in PC4 appear as bright pixels after their dark pixels in Figure 8 above have been enhanced.

The selection of alteration zones by the FPCS method (Figs. 7 and 9) has revealed almost the same locations (see Fig. 9) as those identified by the band ratio images (Fig. 6). Consequently, those locations could be considered potential sites for mineral exploration. A strong correspondence is also visually shown between these inferred alteration zones and the known old artisan gold mining locations in the study areas (Fig. 3).

The spatial distribution of the hydrothermal alteration zones in the study area (Fig. 10) comprising of the iron oxide minerals seen as red and the clay minerals seen in white. Both iron and clay alteration zones (extracted from Fig. 6) have been overlain on an FCC image (bands 7,11,10 RGB) representing silicates in yellow color. Solidification, which is an important indicator of hydrothermal alteration, is not recognizable on VIS and SWIR bands, but instead variations in silica content are recognizable in multispectral thermal infrared TIR images [7].

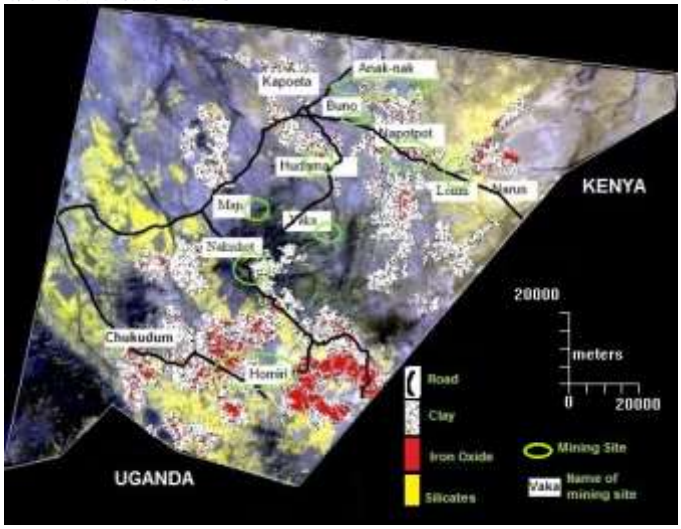

Figure 10. Spatial distribution of hydrothermal alteration zones relative to artisanal mining sites in the study area.

The distribution of the alteration zones corresponds well with seven of the artisanal mining works in the study area except for two sites (Maji and Vaka), which are not associated with alluvial artisanal gold deposits.

The geological features of prime interest for potential mineral prospecting are within the proximity to structures such as fold axis and fault/ shear zones. The results of this study have shown clear association of the detected hydrothermal alteration zones with areas of contact.

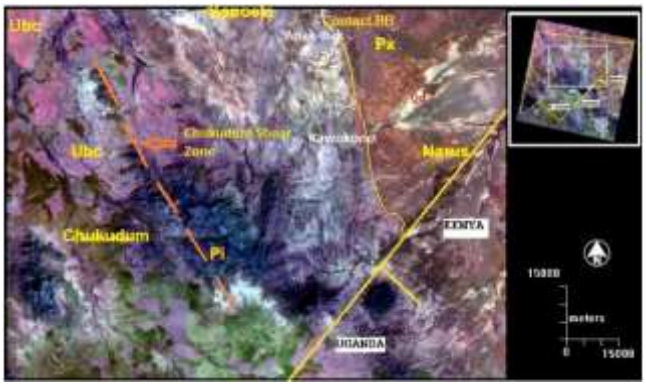

Figure 11. FCC image 475 RGB zoomed-in to the central part of the Didinga Hills for better lithological identification. Ubc is undifferentiated basement complex, Pi is Precambrian intrusive rocks, and Px is Precambrian extrusive rocks.

metamorphism. For instance, the contact BB (Fig. 11) between the extrusive volcanic (Px) and the Schist along which artisanal mining sites (Anak-nak, Napotpot, and Lolim) are located southeast of Kapoeta town and extending to the area SW of Narus town is a clear indication of such association (Figs. 10 and 11).

Other alteration zones are in the vicinity of the shear zone containing artisanal mining sites at Nakishot, Vaka, and Maji. Those associated with faults are in the proximity of Chukudum Shear zone (Fig 11)

5. Discussion

The presence of zones of hydrothermal alteration is reflected by the higher values of OLI band ratios illustrated by lighter tone pixels in the Landsat 8 imagery shown in Figures 6, 7, and 9. Most of these same areas of greater alteration coincide well with areas characterized by significant silicification – quartz veins sometimes associated with sericite and pyrite "unpublished" [3]. For instance, the areas to the east and southeast of Kapoeta town are known as artisan gold mining sites (Fig. 3).

Most artisan gold works are conducted on alluvial deposits, derived from iron-rich rocks suggesting intense surface oxidation that appears widely on the OLI ratio of B4/B2 from the presence of ferric oxides (ilmenites / hematite) (Figs. 6). The mining activities are restricted to areas of mainly weathered or altered metasediments, e.g. marble and tremolite-actinolite schists "unpublished" [3]. Other rock units which include mining activity comprise graphitic gneiss and chlorite-sericite schist with interfoliated quartz veins "unpublished" [3]. Similarly, the band ratio B6/B7 refers to clay minerals of which Kaolinites were the most abundant in the area as shown in Figure 9.

The PCA technique helped in identifying iron and clay minerals, but was not definitive in discriminating or naming the various possible minerals which may constitute the brighter color shown by a particular group of pixels at a specific location on the image. The lithological discrimination by remote sensing does not delineate sharp boundaries, but Rather gradational ones. That is because mapping in this case depends on color recognition which could be blur or obscure due to lose floats or soil stains washed from one rock unit to another [7] [12].

The validity of the applied remote sensing techniques was performed on published and unpublished geological maps, as well as the known sites for artisanal mine conducted by the natives of the Didinga Hills (Fig. 3).

Given the fact that South Sudan has been under-surveyed geologically this study has been utilized in allocation of minimal exploration concessions based on the identified hydrothermal alteration zones as shown on Figure 12 below.

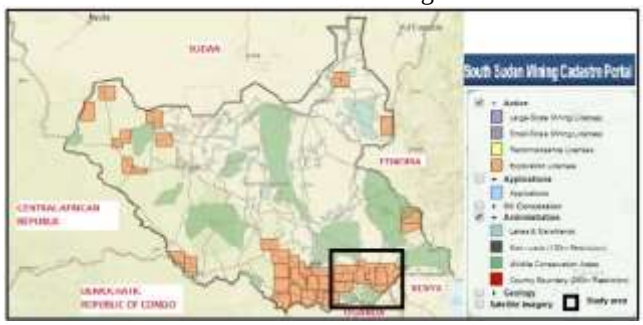

Figure 12. South Sudan Mining Cadastre Portal showing mineral titles concessions (brown polygons) and the study area marked by a black polygon.

Following this research, the study area was granted to mining companies some of which conducted high resolution geophysical together with limited geological and geochemical surveys in their concessions resulting in identification of important targets e.g. granite terrains, greenstone belts, anomalous areas at Anak-nak and Kawokono (Fig. 11). Additionally, some structures e.g. Chukudum Shear Zone and a variety of faults and folds associated with alluvial and eluvial gold occurrences have been recommended for further exploration work.

6. Conclusions

The study focuses on the spatial distribution of the main types (Fe Oxide and Al hydroxyl) of hydrothermally altered rocks as a means of determining the general extent of potential mineralization in the Didinga Hills. The results obtained have identified hydrothermal alteration zones in the Didinga hills. The demonstrated approach has the potential to reduce the cost and time of the preliminary stage of ground reconnaissance that is necessary for decision makers in prioritizing their allocation of mineral exploration titles.

Remote sensing techniques hold the potential to provide information needed for socioeconomic planning, identifying natural hazards (such as earthquake faults, areas of landslides); building the nation's infrastructure of roads and highways, railroads, pipelines, utilities, dams and making wiser decisions about land-use and specifically in development of the country mineral resources. Additionally, Landsat images are free so the cost of conducting the needed survey is low; hence the application of remote sensing is economically viable in case of absence or scarcity of geological survey data, such as is currently happening in South Sudan.

Mapping hydrothermal alteration zones in the Didinga Hills by remote sensing techniques would enable future application of this type of analysis to map the under-surveyed regions of South Sudan for further exploration and sustainable development of its mineral resources.

Acknowledgments

The authors are grateful to Prof. Timothy Warner of University of West Virginia, for his invaluable comments and guidance during the early phases of this study. Thanks to the staff of the Ministry of Mining in South Sudan for their continuous support during the study. The great feedback and comments of Prof. Robert K. Vincent of Bowling Green State University are highly appreciated.

References

[1] Brimhall, G. H., Dilles, J., Proffet, J., 2006. The role of geological mapping in mineral exploration, in: Doggett, M.D., Parry, J. R., (Eds.), Wealth creation in the minerals industry: Integrating science, business education: Society of Economic Geologists Special Publication 12, pp. 221–241.

[2] Anderson, S.D., 2005. Preliminary results and economic significance of geological mapping in the Gem Lake area, southeastern Rice Lake belt, Manitoba (NTS52L11 and 14), with emphasis on the Neoarchean Gem assemblage: in Report of Activities 2005, Manitoba Industry, Economic Development and Mines, Manitoba Geological Survey, 104–116.

[3] Hunting Geology and Geophysics Ltd, 1980. Report to Government of the Republic of Sudan, unpublished.

[4] Guilbert, M.J., and Park, F.C., 1986. The Geology of Ore Deposits. W.H. Freeman, New York.

[5] Yetkin, E., Toprak, V., and Suzen, M.L., 2004. Alteration Mapping by Remote Sensing: Application to Hasandağ – Melendiz Volcanic Complex, ISPRS 2004, 12-23 July 2004, Istanbul.

[6] Kujjo, C. P., 2010. Application of remote sensing for gold exploration in the Nuba Mountains, Sudan. Ms. Thesis, Bowling Green State University. Unpublished.

[7] Vincent, R.K., 1997. Fundamentals of geological and environmental remote sensing: Prentice Hall, 370 p.

[8] Abdelsalam, M.G., Stern, R.J., 1996. Sutures and Shear Zones in the Arabian-Nubian Shield. *Journal of African Earth Sciences* 23, 289–310.

[9] Vail, J. R. 1978. Outline of the geology and mineral deposits of the Democratic Republic of the Sudan and adjacent areas. Overseas Geol. Miner. Resour., London, 49, p. 1-67.

[10] Whiteman, A.J., 1970. The geology of the Sudan Republic. Clarendon press: Oxford, 290 p.

[11] Rowan, L.C., Crowley, J.K., Schmidt, R.G., Ager, C.M., Mars, J.C. 2000. Mapping hydrothermally altered rocks by analyzing hyperspectral image (AVIRIS) data of forested areas in the Southeastern United States. *J. Geochem. Explor.* 68, 145–166.

[12] Hubbard, B.E., Crowley, J.K., 2005. Mineral mapping on the Chilean-Bolivian Altiplano using co-orbital ALI, ASTER and Hyperion imagery: Data dimensionality issues and solutions. *Remote Sens. Environ.* 99, 173–186

[13] Zadeh, M.H., Tangestani, M.H., Roldan, F.V., Yusta, I., 2014. Sub-Pixel mineral mapping of a porphyry copper belt using EO-1 Hyperion data. Adv. Space Res. 53, 440–451.

[14] Zhang, T., Yi, G., Li, H., Wang, Z., Tang, J., Zhong, K., Li, Y., Wang, Q., Bie, X. 2016. Integrating Data of ASTER and Landsat-8 OLI (AO) for Hydrothermal Alteration Mineral Mapping in Duolong Porphyry Cu-Au Deposit, Tibetan Plateau, China. *Remote Sensing*, 8, p.890.

[15] Chavez, P.S., Berlin, G.L., and Sowers, L.B., 1982. Statistical method for selecting Landsat MSS ratios. *Journal of Applied Photographic Engineering*, 8, 23-30.

[16] Corosta A.P., and Moore J. M., 1989. Enhancement of Landsat, Thematic Mapper imagery for residual soil mapping in SW Minas Gerias state, Brazil: a prospecting case history in Greenstone belt terrain. Proceeding of the Ninth Thematic conference on Remote Sensing for Exploration Geology, Calgary, Alberta, Canada, 2-6 October, 1173-1187.

[17] Jensen, J.R., 2005. Introductory Digital Image Processing: A Remote Sensing Perspective, 3rd Edition, Upper Saddle River: Prentice-Hall, 526 p.

[18] Sabine, C., 1999. Remote sensing strategies for mineral exploration: In Remote Sensing for the Earth Sciences—Manual of Remote Sensing, 3rd edn: A. Rencz (ed.) (New York: American Society of Photogrammetry and Remote Sensing. John Wiley and Sons, 375– 447.

[19] Ren, D. and Abdelsalam, M.G., 2001. Optimum Index Factor (OIF) for ASTER data: examples from the Neoproterozoic Allaqi Suture, Egypt. In: Proceeding of the Geological Society of America (GSA), Annual Meeting, Boston, USA, Paper No. 123-0, November 5-8.

[20] Vincent, R.K., Thomson, F., Watson, K., 1972. Recognition of exposed quartz sand and sandstone by two-channel infrared imagery. *J Geophys Res.* 77, 2473–2477.

[21] Goetz, A.F.H., 1989. Spectral Remote Sensing in Geology, Theory and Applications of Optical Remote Sensing, Asrar, G., (edi), John Wiley and Sons, 491-526.

[22] Sabins, F. F.,1997. Remote Sensing Principles and Interpretation. W. H. Freeman Company, New York. 494 p.

[23] Abrams, M.J., Ashley, R., Rowan, L., Goetz, A., and Kahle, A., 1977. Mapping of hydrothermal alteration in the Cuprite Mining District, Nevada, using aircraft scanner images for the spectral region 0.46 to 2.36 pm, *Geology*,5,713-718.

[24] Han, T., and Nelson, J., 2015. Mapping hydrothermally altered rocks with Landsat 8 imagery: A case study in the KSM and Snowfield zones, northwestern British Columbia. In: Geological Fieldwork 2014, British Columbia Ministry of Energy and Mines, British Columbia Geological Survey Paper 2015-1, 103-112.

[25] Hatcher, L. and Stepanski, E., 1994. A step-by-step approach to using the SAS system for univariate and multivariate statistics. Cary, NC: SAS Institute Inc.

[26] Loughlin, W.P., 1991. Principal Component Analysis for alteration mapping. *Photogrammetric Engineering and Remote Sensing*, 57, 1163-1169.

[27] Crosta, A.P., and Rabelo, A., 1993. Assessing of Landsat TM for hydrothermal alteration mapping in central western Brazil. Proceedings of Ninth Thematic conference geologic remote sensing Pasadinea, p. 1053-61, California, USA.

[28] Crosta, A.P., De Souza Filho, C.R., Azevedo F., and Brodie, C., 2003. Targeting key alteration minerals in epithermal deposits in Patagonia, Argentina, using ASTER imagery and principal component analysis. *Int. J. Remote Sens.*24, 4233-4240.

[29] Harris, J.R., Rencz, A.N., Ballantyne, B., and Sheridon, C., 1998. Mapping altered rocks using Landsat TM and lithochemical data: Sulphurets-Brucejack Lake District, British Columbia, Canada. Photogrammetric Engineering & Remote Sensing, 64, 4, 309-322.

Biographies

Cosmas Kujjo received the B.Sc. degree in Geophysics from Cairo University, Cairo, Egypt, in 1985, M.Sc. degree in Geology from the University of Khartoum, Khartoum, Sudan, in 2001, another M.S. degree in Earth Sciences from the Bowling Green State University, Ohio, USA, in 2009, and is a Ph.D. candidate at the University of Kentucky, Lexington, USA, respectively.
His research interests are in Geophysics and Remote Sensing. The Author may be reached at
Cku222@uky.edu

Liang Liang received the B.S. degree in Geochemistry from the University of Nanjing, China, in 1999, M.S. degree in Quaternary Geology from the University of Peking, China in 2003, and Ph.D. degree in Geography from the University of Wisconsin-Milwaukee, USA, respectively. Currently, He is an associate Professor of Geography at the University of Kentucky. His teaching and research areas include: Bioclimatology, Phenology, Remote Sensing, and Biogeography.
Dr. Liang may be reached at
Liang.Liang@uky.edu

Dhananjay Ravat received the B.Sc. degree in Geology from the Maharaja Sayajirao University of Baroda, India, in 1981, M.S. degree in Geophysics from Purdue University, USA in 1985, and Ph.D. degree in Geophysics from Purdue University, USA in 1989, respectively. Currently, He is a Joint Professor at the University of Kentucky. His teaching and research interests are in geophysics and planetary sciences.
Professor Ravat may be reached at
dhananjay.ravat@uky.edu